Tellus (1997), 49B, 93–111
Printed in UK – all rights reserved

TELLUS
ISSN 0280–6509

On the transport of trace elements into Antarctica using measurements at the Georg-von-Neumayer station

By ULRIKE WYPUTTA*, *Meteorologisches Institut der Universität Hamburg, Bundesstraße 55, D-20146 Hamburg, Germany*

(Manuscript received 6 April 1995; in final form 1 September 1996)

ABSTRACT

Origin and transport of ^{222}Rn, surface ozone, and sea salt measured at the German Antarctic research station Georg-von-Neumayer (GvN) (70°37′S, 8°22′W, 36 m) were investigated together with local meteorological observations and calculated 2-dimensional trajectories. Daily trajectories computed for the years 1984–1989 at 500, 850, and 925 hPa levels are presented and grouped according to different flow sectors at GvN. An analysis of these trajectories indicates that at 500 hPa, westerly flow patterns occur for 70% of the time, more in winter than in summer, with an average velocity of 11 ms^{-1}. Easterly flow occurs less frequently (30%) and is weaker (8 ms^{-1}). Nearly 92% of all trajectories calculated at the 850 hPa level and 97% on the 925 hPa surface indicate easterly flows due to orographic effects of the Antarctic continent. In addition, time series of trace elements measured at GvN were analysed together with local meteorological data and the trajectories to find the source regions of the trace elements. Primary results are that periods with high radon-222 concentrations are mostly connected to cyclones approaching from the South American continent. Most of the maxima of surface ozone and sea salt are also well correlated with cyclonic activities near the Antarctic continent. Furthermore, it is found that the seasonal cycle of trace elements is mostly determined by the annual variation of different trajectory groups.

1. Introduction

Antarctica is supposed to have the cleanest air in the global atmosphere. The continent is nearly completely covered with snow and ice. Due to this permanent snow cover, there are no sources of gaseous and particulate trace substances in the atmosphere, apart from small areas of exposed rocks and local research activities. Since Antarctica has no relevant local sources, trace elements measured in the Antarctic atmosphere must be transported from outside into Antarctica. In this study, gaseous and particulate trace substances measured at the German Antarctic research station Georg-von-Neumayer (GvN) (70°37′S, 8°22′W, 36 m) were considered together with meteorological measurements taken at the same station, remotely sensed sea-ice coverage, and 4-day 2-dimensional back trajectories. The intention of the study is to improve the insight into the origin, transport mechanism, and the annual cycle of the trace elements.

The application of atmospheric back trajectories as a tool employed in interpreting atmospheric chemical data has become a standard practice and is used to get information on the origin and pathway of trace substances measured at the GvN. A modeled 2-dimensional trajectory is an estimate of the transport pathway of a small air parcel at a constant pressure level (Kahl et al., 1989). Here, daily trajectories were calculated for the years 1984–1989 and were used to describe flow patterns for GvN in 500, 850, and 925 hPa levels.

* Present affiliation: Universität Bremen, Fachbereich 5, Postfach 330440, D-28334 Bremen, Germany.

Trajectories were manually grouped according to wind speed and direction and stratified by month to consider seasonal changes in the wind regime and therefore the transport of trace elements into Antarctica (Harris, 1992).

Time series of trace elements were analysed together with local meteorological data and the trajectories. Due to their different sources and sinks, radon-222 (^{222}Rn), surface ozone, and sea salt were chosen for this analysis. ^{222}Rn is a mean to study long-range transport processes in the troposphere. It is outgassed from the surface of the surrounding continents, since Antarctica is almost totally ice covered and is therefore an indicator for continental air masses (Polian et al., 1986; Lambert et al., 1990; Pereira, 1990). Measurements reveal high radon activity episodes known as "radonic storms" which are attributed to the rapid transport of continental air into Antarctica.

Ozone is one of the most important trace gases in determining the radiation budget and it is also a precursor for highly reactive radicals. Tropospheric ozone variations in the Antarctic region have been interpreted in terms of air transport processes (Wexler et al., 1960; Oltmans and Komhyr, 1976; Winkler et al., 1992). To clarify the correlation of rapid ozone increases at GvN and the atmospheric conditions, case studies are performed.

The main Antarctic aerosols monitored at GvN are sea salt particles (Wagenbach et al., 1988). They are produced by wind-induced bubble bursting at the ocean surface (Eriksson, 1959; Blanchard, 1985; Wu, 1988) and for an Antarctic coastal station, they are primary aerosols of local origin. Sea salt episodes were investigated and the annual variation of sea salt was also analysed, together with remotely sensed sea ice coverage.

2. Data and trajectory model

2.1. *Trajectory model*

4-day back trajectories were calculated for the GvN with a 2-dimensional model of the Norwegian Meteorological Institute (NMI). NMI used a rectangular grid with a horizontal resolution of 150 km (Heintzenberg and Larssen, 1983). For Antarctica, the model was bounded by the South Pole, 41°S 90°W, 24°S 45°W, and 41°S 5°E to calculate trajectories from westerly directions. At the 500 hPa level, these are trajectories belonging to group NW and SW (Fig. 1) and at 850 and 925 hPa, to group 1 (Fig. 2). To compute trajectories reaching GvN from easterly directions, the boundaries of the model are the South Pole, 41°S45°W, 24°S0°E, and 41°S50°E. Groups NE and SE in Fig. 1 and groups 2 and 3 in Fig. 2 comprise these easterly trajector-

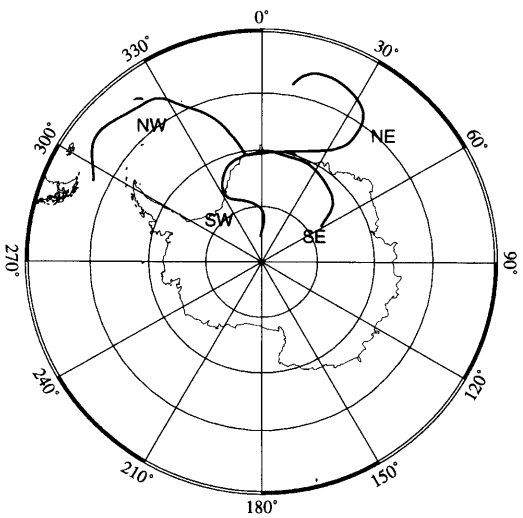

Fig. 1. Trajectory classification at 500 hPa level; trajectories are examples for each group.

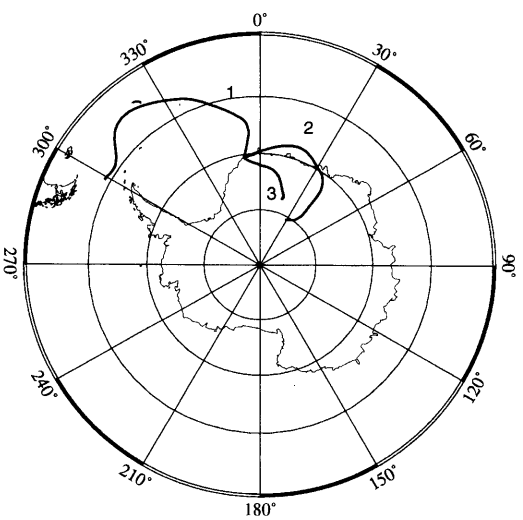

Fig. 2. Trajectory classification at 850 and 925 hPa level; trajectories are examples for each group.

ies. When a trajectory leaves of this area, the calculation is stopped, but this happened in only 5% of all trajectory calculations. The time step for the trajectory calculation is 2 h and the computation is based on the method described by Petterssen (1956), assuming that the motion is strictly horizontal. This assumption of isobaric flow is often unrealistic for long-range transports, but the problem might be assessed by running the model at several pressure surfaces (Kahl et al., 1989). In this study, trajectories were computed at the 500, 850, and 925 hPa levels. The 500 hPa surface was chosen to represent flows in the middle troposphere. Trajectories at 850 hPa represent transports above the planetary boundary layer and trajectories at 925 hPa represent the flow in the boundary layer.

2.2. *Meteorological data*

Surface measurements. Routine surface measurements of meteorological parameters are done at GvN which is located on the Ekström ice-shelf 7 km from the ice-edge facing the open sea during austral summer. The position of the station is between the low-pressure belt surrounding Antarctica at approximately 65°S and the high-pressure region over the central Antarctic continent. The meteorological surface measurements averaged over the period 1984–1989 show a mean surface pressure of about 986 hPa. Surface winds are mainly blowing from easterly directions with an annual mean wind speed of 8 ms^{-1}. The averaged 2 m temperature is −16°C with a maximum of −1°C during summer time and a minimum of −45°C during winter time.

Upper wind data. To compute isobaric back trajectories, the model utilizes zonal and meridional wind components as derived from fields of the European Centre for Medium Range Weather Forecasts (ECMWF). For the years 1984–1989, analysis of these data only for 00 GMT are available at the German Climate Computing Center (DKRZ) in Hamburg. The wind components were produced on 2.5° grids on the standard pressure surfaces. For a calculation of the trajectories, spatial and temporal interpolations are necessary to obtain wind components at every grid point and for every time step.

Since wind fields from the ECMWF analyses are the basis of the trajectory computation, it is necessary to check their quality in a region like Antarctica where the coverage with upper air radiosondes is very limited. Hence, a comparison between ECMWF wind fields and the radiosonde winds at GvN will give information on the quality of the ECMWF data.

At the GvN radiosonde, observations are usually made once a day. For 1984–1989, 78% of all wind data at 500 hPa, 77% at 850 hPa, and 70% at 925 hPa are available. ECMWF winds are available for each day, but for this comparison, the data set is reduced and wind data are interpolated from the nearest grid points of the 2.5° grids to the position of GvN. Both data sets are not independent, as radiosonde observations at GvN are included in the ECMWF analyses. Daily ECMWF wind fields are calculated for 00 GMT, while radiosonde observations at GvN are taken at 09 GMT, so these data have a great temporal difference.

At 500 hPa, the local radiosonde measurements show the strongest winds of 35–45 ms^{-1} with southwesterly to westerly directions (Fig. 3). High wind speeds are also measured with easterly flows. The wind data calculated from ECMWF wind fields show a similar picture. Strong wind speeds are obtained at easterly and southwesterly to westerly directions, but the wind speed of the ECMWF analyses is lower than that measured with radiosondes (Fig. 3). This seems reasonable, because ECMWF analyses represent an average value over a surface, whereas winds measured with radiosondes are point measurements.

At the 850 and 925 hPa levels, 2 maxima of wind speed measured by radiosondes are found. The strongest winds up to 40 ms^{-1} at 850 hPa and up to 35 ms^{-1} at 925 hPa appear at easterly directions are due to cyclones passing the station (Gube-Lenhardt and Obleitner, 1986). This main wind direction in the boundary layer is also present in the data fields of ECMWF analyses where the winds are not so strong due to the averaging process. A 2nd maximum of wind speed measured from radiosondes is found at southwesterly directions. This maximum is attributed to synoptic depressions which have their centres south of the station (Gube-Lenhardt, 1987), but is not represented in the ECMWF data.

2.3. *Trace elements*

Time series of trace elements were analysed together with local meteorological data and tra-

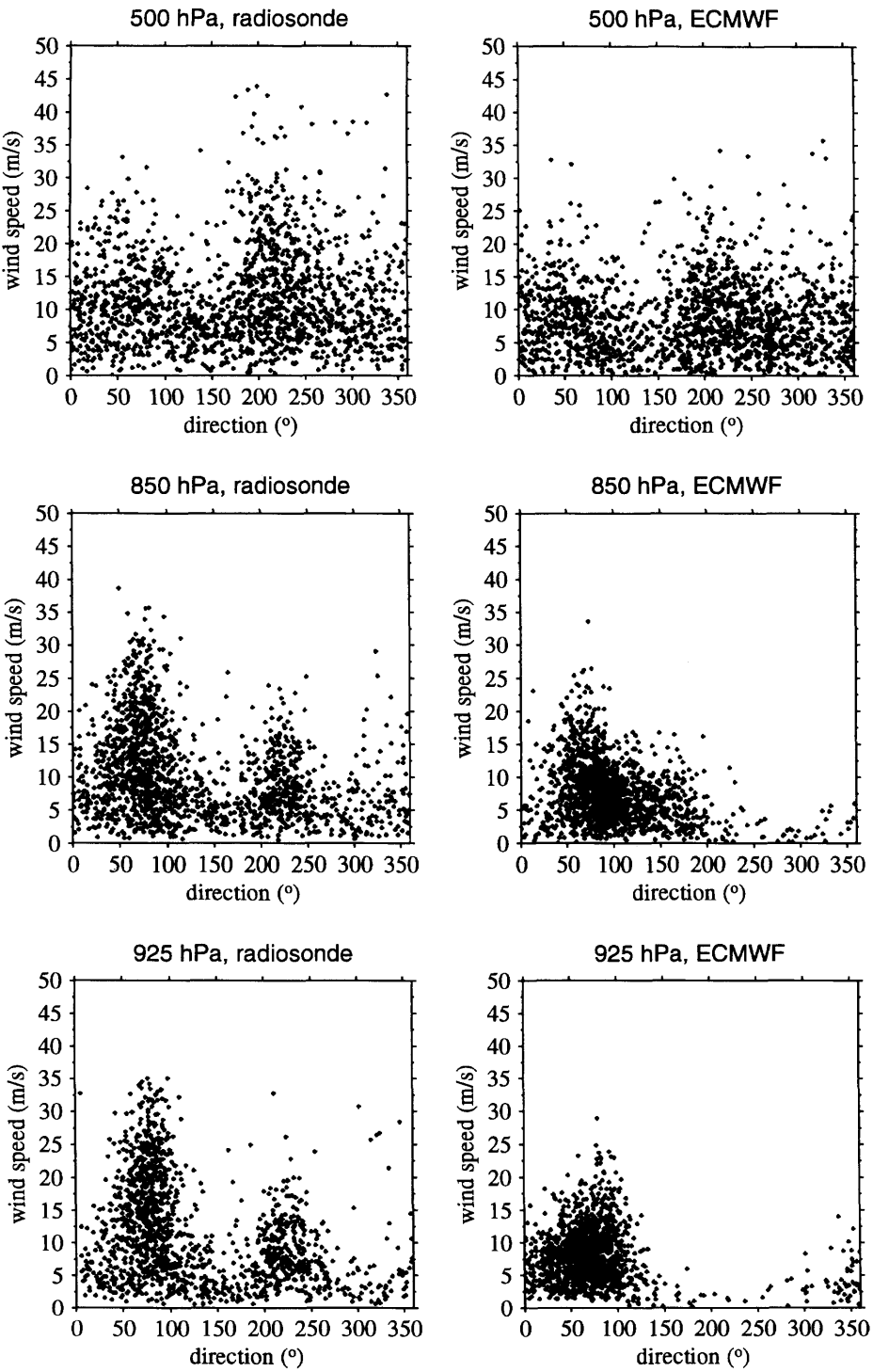
500 hPa, radiosonde
500 hPa, ECMWF
850 hPa, radiosonde
850 hPa, ECMWF
925 hPa, radiosonde
925 hPa, ECMWF
wind speed (m/s)
direction (°)
0 5 10 15 20 25 30 35 40 45 50
0 50 100 150 200 250 300 350

jectories. Because of their different sources and sinks, ^{222}Rn, surface ozone, and sea salt were chosen for this analysis.

Radon-222. The radioactive noble gas ^{222}Rn constitutes a unique tracer of atmospheric transport processes. It is a decay product of uranium-238/radon-222, and is outgassed from the surface of the continents, except from Antarctica which is almost totally ice covered (Polian et al., 1986; Lambert et al., 1990; Pereira, 1990). The outgassing rate depends on soil characteristics such as ^{238}U/^{222}Rn content, porosity, moisture content, snow cover, and local meteorological conditions (Turekian et al., 1977). The mean emission rate is approximately 0.7 atoms cm^{-2}s^{-1} (Lambert et al., 1982). In contrast, the outgassing rate of the sea surface is about 100 times less (Wilkening and Clements, 1975). As a noble gas, ^{222}Rn is chemically inert and disappears from the atmosphere only by radioactive decay with a 3.8 day half-life period. Since Antarctica has no sources of ^{222}Rn, the atmospheric ^{222}Rn concentrations in Antarctic areas are controlled by their long-range transport from mid-latitudes that varies with the season.

^{222}Rn activity measured at GvN is archived at the Institute of Environmental Physics in Heidelberg, Germany. The daily ^{222}Rn activity at GvN during 1984–1989, calculated with α-spectroscopy of ^{210}Pb decay, varied between 0.001 and 0.084 Bq m^{-3}, with an average of 0.026 ± 0.010 Bq m^{-3}. The main feature of the concentration record is the existence of rapid and sharp ^{222}Rn episodes. These high ^{222}Rn variations sometimes attained 0.08 Bq m^{-3} and are called "radon storms" which are attributed to the rapid transport of continental air into Antarctica (Fig. 4).

Surface ozone. Another gas observed at GvN is surface ozone that is in a pristine atmosphere of stratospheric origin and is introduced into the troposphere by stratosphere-troposphere exchange processes and finally destroyed at the earth's surface. Variations of tropospheric ozone in the Antarctic region have been widely interpreted in terms of air transport processes (Wexler et al., 1960; Oltmans and Komhyr, 1976; Winkler et al., 1992). At GvN, surface ozone is measured with the wet chemical KJ method (Attmannspacher, 1971) and the data are available at the Meteorological Observatory Hamburg, Germany. Daily averages of ozone partial pressure varied between 0.2 and 3.3 mPa (1982–1986) and reached up to 4.4 mPa in the year 1987 (Fig. 4), corresponding to measurements at other coastal Antarctic stations (Oltmans, 1981; Murayama et al., 1992; Gruzdev et al., 1993). One of the dominating features of the temporal variability of Antarctic surface ozone is its annual variation, with a broad winter maximum and a small summer minimum with a range equal to about 50% of the average annual concentration.

Sea salt. The main component of the Antarctic aerosols monitored at GvN are sea salt particles (Wagenbach et al., 1988). Sea salt particles are produced by wind-induced bubbles bursting at the ocean surface (Eriksson, 1959; Blanchard, 1985; Wu, 1988), and for an Antarctic coastal station, they are primary aerosols of local origin. Aerosol nuclei are sampled on cellulose filters and sea salt concentrations are calculated from Na or from Cl if no Na data are available (Wagenbach et al., 1988). These aerosol data are available at the Institute of Environmental Physics in Heidelberg, Germany. The sampling period was 2–3 weeks which is seen from Fig. 4. The sea salt density at GvN reached values up to 5000 ng m^{-3} and the weighted mean during 1984–1989 is 980 ng m^{-3}.

Beryllium-7. Like ozone in the pristine atmosphere, beryllium-7 (^{7}Be) is of stratospheric origin only, hence, the activity of ^{7}Be measured at GvN was investigated in connection with surface ozone. ^{7}Be is produced by interaction of secondary cosmic rays with nitrogen and oxygen nuclei (Lal and Peter, 1967) and has a half-life of 53.2 days. It is an atmospheric tracer and can be used as an indicator for stratospheric-tropospheric exchange. At GvN, ^{7}Be is sampled on cellulose filters with a period of 2–3 weeks like sea salt and the ^{7}Be activity is calculated using a large HPGe p-type

Fig. 3. Wind speed as a function of direction at GvN measured by radiosondes and analysed from ECMWF fields at levels of 500, 850, and 925 hPa.

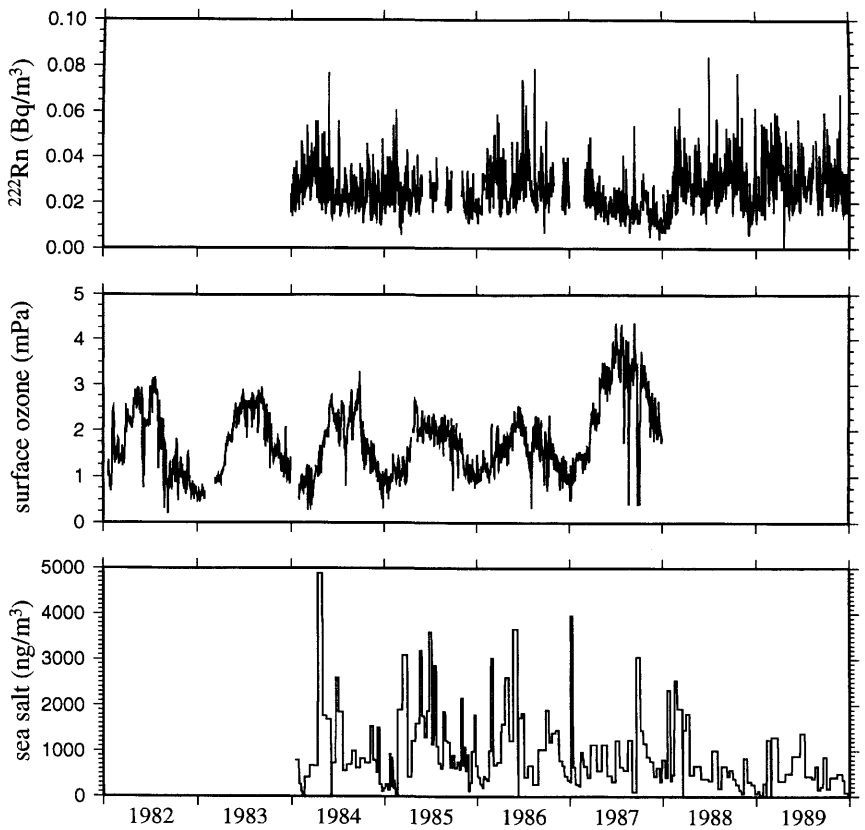

Fig. 4. Time series of ^{222}Rn activity, surface ozone partial pressure, and sea salt density.

coaxial detector (Wagenbach et al., 1988). Monthly mean values of ^{7}Be averaged over the years 1984–1987 were between 3.5 and 5.8 mbq m^{-3}. These data are also available at the Institute of Environmental Physics in Heidelberg, Germany.

2.4. Sea ice

To determine the sea ice concentration around Antarctica, data of remotely sensed sea ice coverage available at the National Snow and Ice Data Center (NSIDC) at the University of Colorado, Boulder, Colorado, were used. The sea ice concentration was calculated from the brightness temperatures measured with the Special Sensor Microwave/Imager (SSM/I) using a technique of Cavalieri et al. (1984). Ice concentrations are given in units of % and range from 0–100% on a 50-km grid, averaged from 4 adjacent 25-km grid cells. The sea ice coverage data have been available once a day since July 1987.

3. Trajectories

A trajectory is best used as an indication of the general airflow rather than the exact pathway of an air parcel. The analysis of a large number of trajectories in a climatological sense will reduce the effects of individual errors so that a reasonable representation of the airflow to GvN is possible. A major disadvantage of the isobaric trajectory model used in this paper is the assumption that the flow follows constant pressure surfaces so that the vertical motion is minimal. The severity of this problem can be assessed by running the model at several pressure surfaces (Kahl et al., 1989). For

the purpose of preparing a climatology of relative patterns of transport to GvN, the procedure of calculating isobaric trajectories was determined to be adequate (Moody and Galloway, 1988).

Uncertainties in trajectories also result due to uncertainties in the wind field over data-sparse regions. Kahl et al. (1989) estimated the uncertainty of trajectories produced for the Arctic, a similar data-sparse region like the Antarctic. They calculated 5-day back trajectories at the 850 and 700 hPa levels using 3 large-scale trajectory models and 2 different meteorological data bases. The models employ different parameterizations of vertical motions, inter alia, an isobaric model. After 5 days, the median horizontal displacements between the trajectory endpoints were mostly in the 800–1000 km range. These uncertainties were more caused by the model sensitivity to the meteorological data than to different parameterizations of motions. Due to the fact that the trajectory model of the NMI used in this paper is also an isobaric one and trajectories were calculated for an Antarctic station which lies in a data-sparse region, the magnitude of errors of trajectories computed for GvN is expected to be similar to the estimations of Kahl et al. (1989).

For GvN, trajectories were calculated during 1984–1989 for each day on 3 pressure surfaces, 500, 850, and 925 hPa. Trajectories at 500 hPa represent flows in the middle troposphere. Computations for 850 hPa show the transport above the boundary layer, while at 925 hPa, flow patterns in the boundary layer can be investigated. To describe flow patterns for GvN, trajectories are grouped manually according to different directions. Two different kinds of classifications were chosen for trajectories computed at the 500 hPa level and for those calculated at the 850 and 925 hPa surfaces. At 500 hPa, all trajectories running north of 70°S and west of 0°E were included in group NW, south of 70°S and west of 0°E in group SW. Trajectories having their origin east of 0°E belong to the 2 easterly groups, whereas trajectory pathes north of 70°S were included in group NE and south of 70°S in group SE. At 850 and 925 hPa levels, all trajectories having their origin west of 0°E belong to group 1. Easterly trajectories were included in classes 2 and 3, where a distinction between trajectory paths over land and sea and those only over land was made. All daily trajectories on the 3 levels for all groups were noted and summarized by year and month. In Figs. 1 and 2, examples for each group are shown.

3.1. Trajectories at 500 hPa

Trajectories computed at the 500 hPa level were grouped into 4 different classes and examples for each group are shown in Fig. 1. The first class, named NW, contains trajectories coming from the northwest of GvN. These trajectories represent the preferred route of cyclones from South America and the Weddell Sea. 40% of all trajectories at the 500 hPa level belong to this group (Table 1). This can be explained with the location of GvN lying between the circumpolar trough and the permanent high pressure over the central Antarctic continent. The average wind speed in this trajectory class is 13 ms^{-1}, being higher than in the other groups; hence, the most long-range transports to GvN are attributed to this trajectory group.

Trajectories reaching GvN from southwesterly directions are collected in the next most frequent group (31%), class SW. These flows are often anticyclonic and transport air from the Antarctic continent to GvN. Otherwise, this trajectory group represents mesoscale lows over the Weddell Sea. The average speed of these trajectories is 8 ms^{-1}.

The last 2 groups, NE and SE, indicate trajectories reaching GvN from northeasterly and southeasterly directions. Northeasterly flow patterns (NE) are consistently cyclonic and reflect storms like class NW. Due to the atmospheric circulation,

Table 1. *Frequency and wind speed with standard deviations of trajectories at 500 hPa calculated for 1984–1989*

	NW	SW	NE	SE
Frequency	40±3%	31±3%	16±2%	13±2%
Wind speed	13±6 ms^{-1}	8±4 ms^{-1}	8±4 ms^{-1}	7±3 ms^{-1}

only 16% of all trajectories calculated in 500 hPa belong to this group with an average speed of 8 ms^{-1}. 13% of all trajectories are assigned to group SE and represent anticyclonic flow and have their origin over the Antarctic continent. They describe transports of continental air with the weakest average wind speed of 7 ms^{-1}.

Westerly flows at the 500 hPa level are most frequent and occur nearly 71% of the time, due to the westerly circulation of the atmosphere. These flows are strong at 11 ms^{-1}, whereas easterly flows are generally weaker at 8 ms^{-1} and less frequent (29% occurrence). Similar results are also found by Harris (1992), who computed trajectories at the 500 hPa surface for the South Pole station.

The frequencies of all trajectory classes show seasonal variations. This can be seen in Fig. 5. At 500 hPa, the most frequent trajectory group is the NW group. Fig. 5 shows a smaller frequency in summer (December–February), up to 18% in February, and higher frequencies during autumn, winter, and spring. For this group, the pathway of cyclones describes the higher frequency of this trajectory group, and represents the migration of the circumpolar trough to the south in autumn (Taljaard, 1967; Schwerdtfeger, 1984). This causes an increase of cyclonic activity at GvN and an increase of the frequency of the NW trajectory group.

As well as the frequencies of trajectories, the flow velocities show a seasonal variation. In summer, when the circumpolar trough is far away from GvN, the flows have the smallest velocities near 10 ms^{-1}. During autumn, winter, and spring, the wind speed is much stronger, and the strongest transports, and therefore the longest pathways, occur during July with a speed of 15 ms^{-1}. As shown in the Fig. 5, the frequency of the NW trajectory group has a minimum in February which represents a minimum of cyclonic activity at GvN. In this month, flow patterns from southwesterly directions are dominant at 500 hPa. They are often anticyclonic and of smaller wind speed (7 ms^{-1}). During autumn and winter, the frequency of flow patterns from the southwest is nearly 30% and the velocity of flows increases up to 11 ms^{-1}, which indicates cyclonic flows from the Weddell Sea. In October, there is a second frequency maximum with an average velocity of 9 ms^{-1}, and anticyclonic flow patterns are dominant.

The NE group shows frequency maxima in summer due to the northern position of the circumpolar trough during summer, when cyclones can reach GvN from northern directions (Taljaard, 1967). In the winter time, the movement of cyclones tends more to easterly directions, so an approach to GvN occurs less frequently and the NE group has a minimum during this season. The seasonal variation of wind speed in flow patterns from the northeast also shows reduced values during summer of about 6 ms^{-1} and stronger flows during winter.

Trajectories from the southeast do not show seasonal variations. These flows occur during the whole year with a frequency of almost 10% and transport air masses from the Antarctic continent to GvN. Only for December is a weak maximum due to the minimum of cyclonic activity at GvN recognizable. This group has the weakest winds and therefore the shortest transports. In contrast to the trajectories, the wind speed shows a seasonal variation with low wind speeds in summer (5 ms^{-1}) and stronger transport in winter (9 ms^{-1}).

The seasonal variation of trajectory frequencies in each group represents the weather situations at GvN. Because of the position of the station lying near the low pressure belt surrounding Antarctica at approximately 65°S, cyclonic flows from westerly directions dominate the flow pattern during autumn, winter, and spring, and anticyclonic flows rarely occur. In summertime, the circumpolar trough lies more to the north and the movement of cyclones changes so that an approach of cyclones from northeasterly directions occurs more frequently while the transport of air from the northwest has a minimum. During summer, anticyclonic flows are dominant from the southeast as well as from southwesterly directions.

3.2. Trajectories at 850 and 925 hPa

Trajectories calculated on the 850 and 925 hPa surfaces are grouped in the following way. The

Fig. 5. Frequency and wind speed with standard deviation for different trajectory groups at the 500 hPa level averaged over the years 1984–1989.

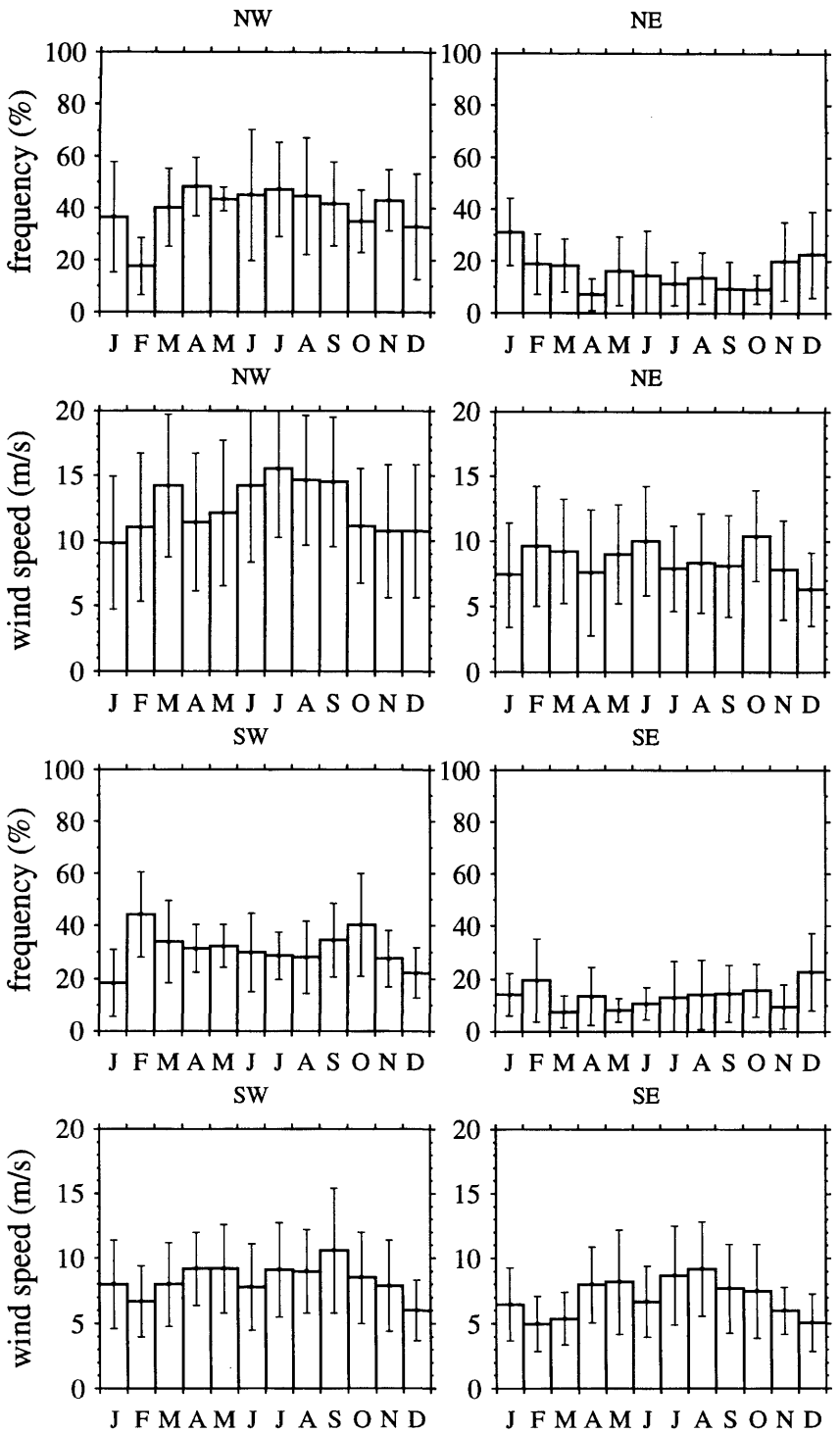
NW
NE
frequency (%)
100
80
60
40
20
0
J F M A M J J A S O N D
NW
NE
wind speed (m/s)
20
15
10
5
0
J F M A M J J A S O N D
SW
SE
frequency (%)
SW
SE
wind speed (m/s)

Table 2. *Frequency and wind speed with standard deviations of trajectories at 850 and 925 hPa calculated for 1984–1989*

	Group 1	Group 2	Group 3
850 hPa			
Frequency	8±3%	33±8%	59±10%
Wind speed	10±3 ms^{-1}	6±2 ms^{-1}	5±2 ms^{-1}
925 hPa			
Frequency	3±2%	34±10%	63±10%
Wind speed	9±3 ms^{-1}	6± 2 ms^{-1}	5±2 ms^{-1}

first group contains all trajectories reaching GvN from northwesterly directions (group 1 in Fig. 2). These flows are the strongest with an average wind speed of 10 ms^{-1}, but only 8% at 850 hPa and 3% at 925 hPa (Table 2) of all trajectories belong to this class. Most of the low-level trajectories, 82% at 850 hPa and 97% at 925 hPa, indicate easterly flows in and above the boundary layer. These easterly flows are divided into trajectories that pass the ocean and the Antarctic continent (group 2), and those that transport only continental air to GvN (group 3). Trajectories of group 2 extend parallel to the coast due to orographic effects. At the 850 hPa surface, 33% of all trajectories and at the 925 hPa level, 34% belong to group 2. These trajectories show a transport of marine air to GvN with an average wind speed of 6 ms^{-1} at both levels. The most frequent group is class 3, which contains trajectories transporting continental air to GvN. This group occurs at 850 hPa for 59% and at 925 hPa for 63% of the time. These flow patterns are not so strong and the transports on both surfaces have average wind speeds of 5 ms^{-1}.

Trajectories reaching GvN from southwesterly directions do not exist at the 850 and 925 hPa levels. The absence of such a group might be explained with the wind fields analysed from ECMWF, which are used to compute the trajectories. These data sets never show wind components from the southwest.

In the 850 and 925 hPa surfaces, group 1 contains trajectories reaching GvN from northwesterly directions. The seasonal variation of trajectory group 1 is shown in Fig. 6. Group 1 has a similar behaviour as group NW at 500 hPa with a frequency minimum in summer and a weak maximum during winter representing the cyclonic activity at GvN. Group 2 at 850 (Fig. 6) and

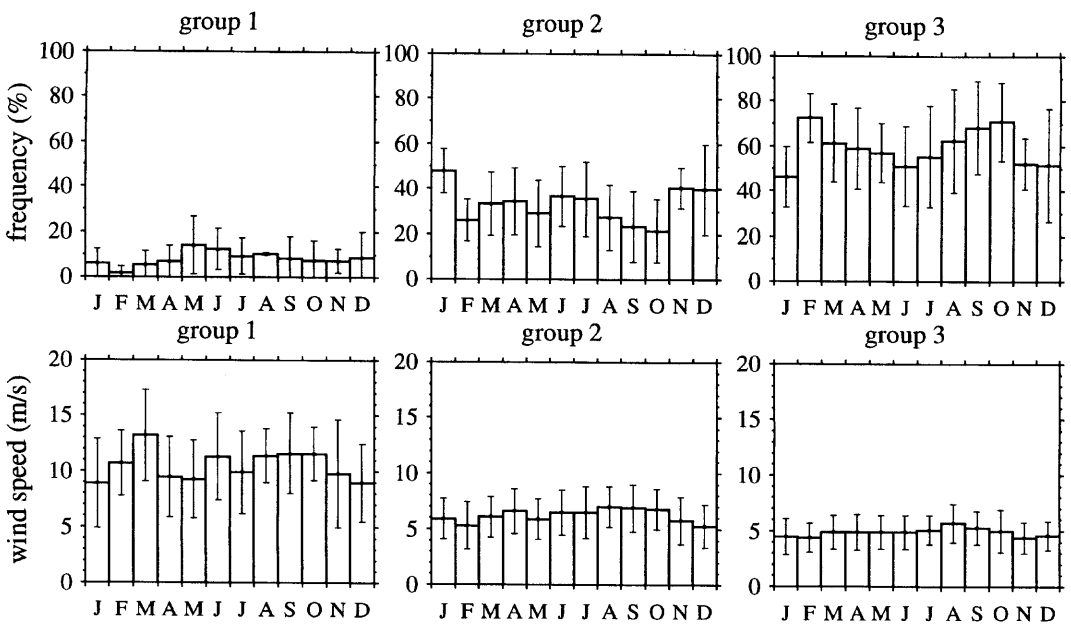

Fig. 6. Frequency and wind speed with standard deviation for different trajectory groups at the 850 hPa level averaged over the years 1984–1989.

925 hPa (not shown) has maximum values in summer and also high frequencies in winter. During summer, trajectories from the northeast at 500 hPa are coupled with trajectories at 850 and 925 hPa, and belong to group 2, and a transport of marine air from easterly directions occurs. In the winter time, low-level group 2 is coupled with trajectory group NW at 500 hPa. The maximum during the winter is clearly caused by an increase of cyclonic activity during this season.

Further on, a transport of continental air at low levels (group 3) occurs together with anticyclonic flows from southwesterly and southeasterly directions at 500 hPa. This occurs most frequently in February and October, whereas during winter, cyclonic flows, with increased frequencies in groups 1 and 2, take place. From November to January, the frequency of group 3 has a minimum, and during this time, most of the trajectories in 850 and 925 hPa belong to group 2 (Fig. 6). Seasonal variations in the average velocity of transport are weak for groups 2 and 3, while for group 1, no annual cycle is found.

It might be questionable to compute trajectories at 850 and 925 hPa pressure levels, since the elevation of the Antarctic continent is high, so that these pressure levels must be beneath ground. Nevertheless, the ECMWF wind fields are available at these pressure levels, because the analysis neglects the orography. A comparison with 3-dimensional trajectories calculated for several days for GvN (Kottmeier, personal communication) showed that the horizontal structure of the 3-dimensional trajectories, which started on the Antarctic continent and ran to GvN, is very similar to the trajectories calculated in this paper. This gives some confidence that the 2-dimensional trajectories at low levels describe the transport of air masses from the Antarctic continent to GvN, at least on a qualitative basis.

4. Trace elements

The previously presented analysis of flow patterns at different pressure surfaces for GvN have shown that different flow regimes depending on the cyclonic or anticyclonic activity exist. It is now straightforward to look at time series of trace elements, their origin, and their pathways into Antarctica. As mentioned earlier, ^{222}Rn, surface ozone, and sea salt were chosen from the trace substances measured at GvN for the analysis, because they have totally different places of origin.

4.1. Radon-222

An analysis of ^{222}Rn activity and local synoptic parameters show that the dependence between temperature, wind speed and direction, and pressure on one side and ^{222}Rn activity on the other side is very weak. Despite this lack of correlation, an increase of ^{222}Rn is often observed with an increase of temperature and wind speed and low atmospheric pressure (Polian et al., 1986; Pereira, 1990). Fig. 7 shows annual variations of ^{222}Rn activity and surface pressure averaged monthly during 1984–1989. It is clearly seen that there exists an anticorrelation between surface pressure and ^{222}Rn activity at GvN. This implies that high ^{222}Rn concentrations are coupled with cyclonic weather events.

An example of a so-called radon storm from the time series of ^{222}Rn is given in Fig. 8, where local meteorological observations at 3-h intervals and daily averaged ^{222}Rn activity, are shown for the period 15–21 August 1986. The daily ^{222}Rn mean activity increased 17 August up to 0.08 Bq m^{-3}. The meteorological data describe the approach and passage of a cyclone at GvN. Before a cyclone arrives at GvN, the wind turns east with increasing speed, surface pressure decreases, and the temperature increases because of the advection of warm air in front of the cyclone. Close to the

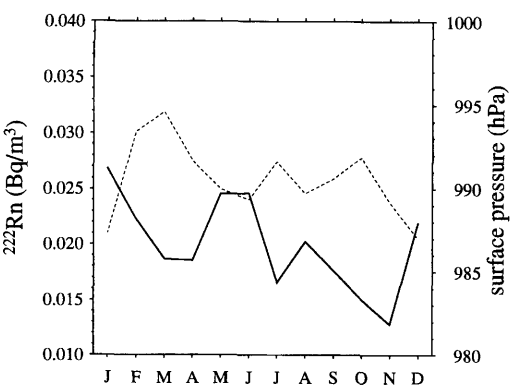

Fig. 7. Annual variability of monthly mean ^{222}Rn activity (solid) and surface pressure (dashed) during the period 1984–1989.

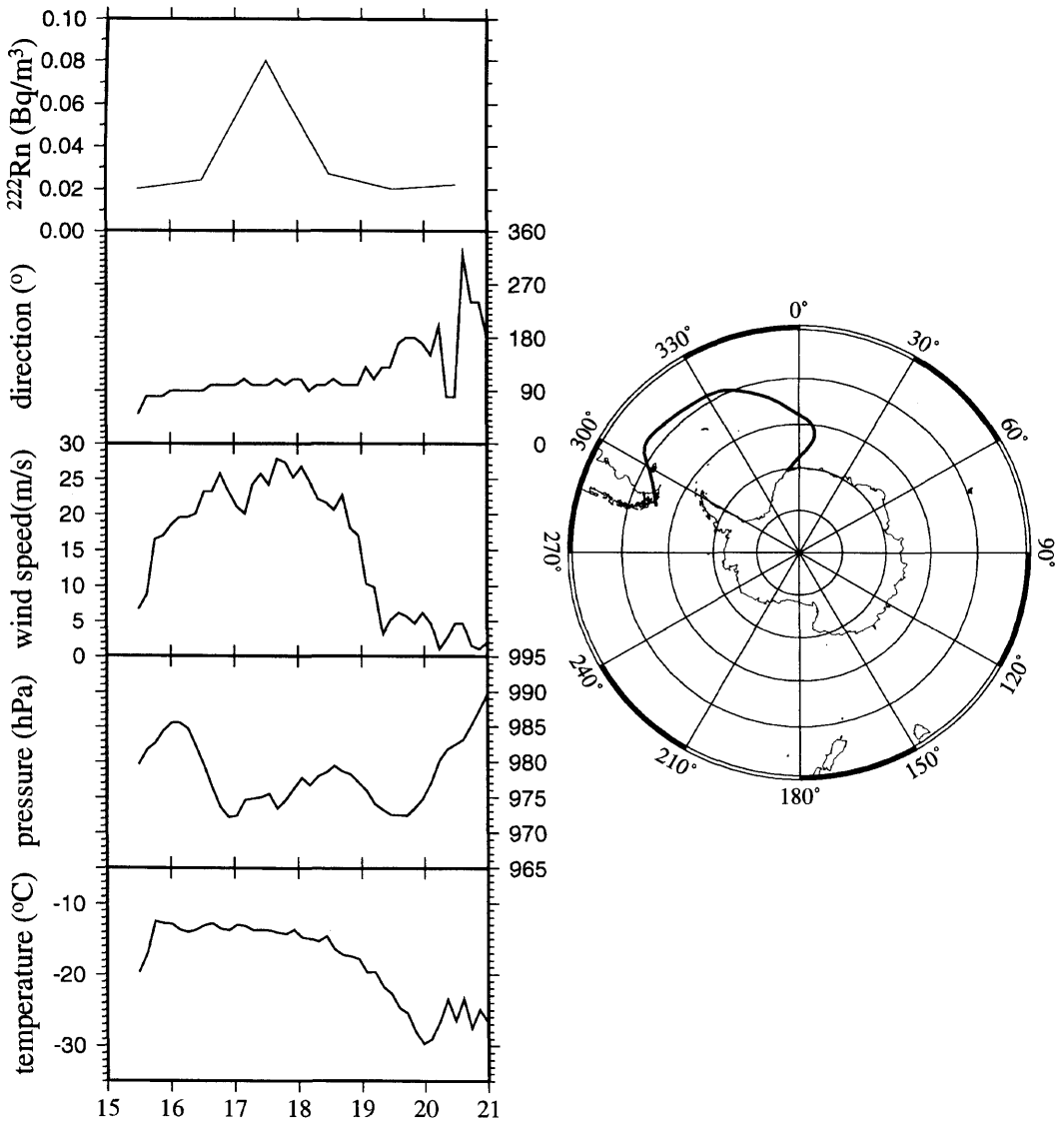

Fig. 8. Local meteorological parameters and ^{222}Rn activity during the period 15–21 August 1986 and the trajectory calculated at the 500 hPa level for 17th August 1986.

cyclone passing, strong easterly wind is measured at GvN with warmer temperature and low surface pressure. Behind the cyclone, the wind turns south-easterly to southwesterly directions, with a decrease of speed and an increase of pressure, while the temperature decreases because of the advection of cold air from the Antarctic continent (Kottmeier, 1988).

All these features are observed 15–21 August 1986. From 15–19 August, the measurements show an easterly flow with a high wind speed of 25 ms^{-1}, low pressure of 975 hPa, and relatively warm temperature of -15°C. During this time, the radon storm occurred and the ^{222}Rn was transported with the cyclone into Antarctica.

A trajectory at the 500 hPa level reached GvN

during the radon storm, 17 August 1986, which belongs to group NW. This trajectory describes the track of the observed cyclone (Fig. 8). The trajectory has its origin over South America on 14 August 1986, and during the transit over the continent, convection above South America transports radon-rich air rapidly from the boundary layer to upper levels. Then, ^{222}Rn was transported by the cyclone to GvN and arrived at the station with the warm front (Winkler et al., 1992). This is reasonable, since ^{222}Rn in the Antarctic originates from low latitudes and should correlate with warm air masses. An analysis for the entire time period 1984–1989 showed that 84% of the observed radon storms are connected with cyclones coming from the South American continent and transporting ^{222}Rn from South America to Antarctica.

A 2nd type of meteorological situation is responsible for the remaining 16% of radon storms. In these situations, a transport of ^{222}Rn occurred with southwesterly winds and cold air in an anticyclonic flow. The corresponding trajectories at a 500 hPa surface reaching GvN on radon storm days have their origin over the Antarctic peninsula, a part of Antarctica which has ice free places.

4.2. *Surface ozone*

In pristine regions like Antarctica, the tropospheric ozone is of stratospheric origin and transported by stratospheric-tropospheric exchange processes from the stratosphere into the troposphere. Therefore, variations of surface ozone can be interpreted in terms of transport processes. A possible candidate as a forcing mechanism for the annual surface ozone variations is the intensity and frequency of synoptic scale disturbances moving from subpolar latitudes into Antarctica (Wexler et al., 1960; Oltmans and Komhyr, 1976). An increase of surface ozone concentrations at GvN is likely caused by weather patterns, where an increase of stratospheric-tropospheric exchange occurs in midlatitudes (Winkler et al., 1992).

At GvN, correlations between local synoptic parameters and the surface ozone partial pressure are not significant, so that case studies of large ozone increases were examined. All day-to-day ozone partial pressure variations during 1984–1987 greater than 0.2 mPa (the average day-to-day ozone variation is 0.15 mPa) were extracted from the time series. 2 types of ozone transport mechanism to GvN are recognizable from the cases examined. An example of the 1st type is shown in Fig. 9, where the increase of the surface ozone partial pressure is coupled with the arrival of a cyclone at GvN. Trajectories calculated at the 500 hPa level for 13 and 14 July 1986 belong to group NW and show the track of a cyclone and transported air, from midlatitudes into Antarctica, as mentioned by Winkler et al. (1992). Ozone is enriched due to stratospheric-tropospheric exchange and arrives at GvN in conjunction with cold air masses behind the cold front. The local meteorological parameters measured every 3 h and daily-averaged surface ozone partial pressures are shown for the time period 6–17 July 1986. In the 1st part of the time series (6–12 July 1986), the meteorological observations show the features of an anticyclonic situation with southeasterly to southwesterly weak winds of nearly 5 ms^{-1}, high pressure, and low temperature. The ozone partial pressure decreased during these 8 days from 2.0 to 1.5 mPa. On 13 July 1986, the wind suddenly turned to the east announcing the next low-pressure system. From 13–17 July 1986, the meteorological data show the approach and passage of a cyclone. The cyclone is indicated in the data set through strong easterly wind speeds (15 ms^{-1}) and high temperatures, which are the consequence of advection of warm air at the front of the cyclone. These findings from the local meteorological data describing the arrival of a cyclone at GvN, confirmed the assumption that the increase of surface ozone partial pressure in pristine regions occurs with synoptic scale disturbances moving from midlatitudes into Antarctica. Examinations of all strong surface ozone partial pressure increases of surface ozone during 1982–1987 showed that this kind of transport mechanism is responsible for 66% of all ozone maxima and happened more often in winter time than in summer time.

The 2nd type of ozone transport mechanism shows an increase of surface ozone with relatively low wind speed from southerly directions, high surface pressure, and low temperature. 2 or 3 days before the ozone partial pressure increased, a cyclone passed GvN which transported ozone in mid-tropospheric levels southward to Antarctica where the air sinks and flows are northerly. This

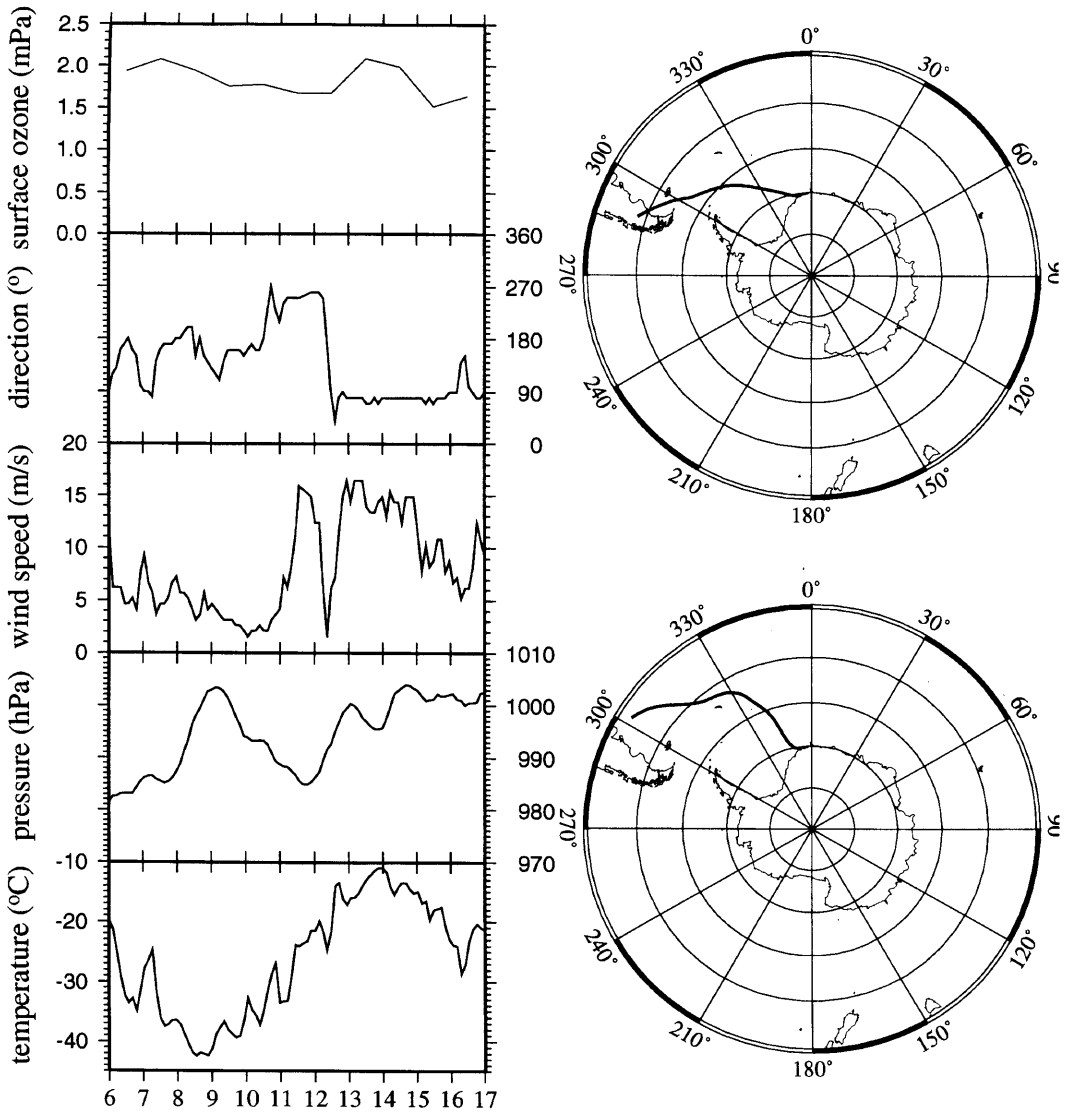

Fig. 9. Local meteorological parameters and surface ozone partial pressure during the period 6–17 July 1986, and the trajectories calculated at the 500 hPa level for 13 July (above) and 14 July 1986 (below).

type of transport is described by Wexler et al. (1960) and is found in the meteorological and surface data measured at GvN in 33% of all ozone maxima.

The time series of surface ozone shows an annual variability with a summer minimum and a maximum in winter (Fig. 4). The analysis of case studies has shown that ozone increases mainly occur with cyclones, more often in winter than in summer, which can be explained by the annual variability of cyclonic activities at GvN. While in autumn, winter, and spring the variability of surface ozone partial pressure is mostly controlled by the frequency of cyclonic activity (Oltmans and Komhyr, 1976), in summer, the time series of ozone has a minimum which cannot be explained

purely by a lack of low pressure systems. The seasonal variability of ^{7}Be activity at GvN (shown in Fig. 10 as monthly averages over the whole period of record) suggests that the downward movement of air from the upper atmosphere to the ground level is more effective in summer than in the remaining seasons of the year (Sanak et al., 1985). To obtain the observed summer minimum, photochemical destruction of ozone must be a very effective process in decreasing the lower tropospheric ozone concentration. A similar conclusion has been drawn by Murayama et al. (1992) for the Syowa Station.

4.3. *Sea salt*

The time series of sea salt (Fig. 4) shows some events where the sea salt concentrations averaged over the sampling period of 2 to 3 weeks are very high. These events occurred mainly in autumn and less often in spring. Analysis of all sea salt events in conjunction with the meteorological data set averaged over the sampling periods reveal that during these periods, one or more cyclones passed GvN. As an example of the meteorological situation during a period with high sea salt density of about 2335 ng m^{-3}, a period from 18–29 January 1988 is shown in Fig. 11. On the 1st day of this period, the meteorological data describe weather conditions with high pressure and low wind speeds with directions from southwest to northwest. During the time from 19–27 January, 2 cyclone passings at GvN with strong easterly winds were observed. Trajectories computed at the 500 hPa level mostly came from northwesterly directions and represent the trail of the cyclones. Analysing sea salt concentration trajectories at the 850 and 925 hPa are more important since the origin of sea salt aerosols in the ocean. They are produced by wind-induced bubble bursting at the ocean surface (Eriksson, 1959; Blanchard, 1985; Wu, 1988) and most of the sea salt particles are found in the lowest 1.5 km of the atmosphere (Eriksson, 1959). Hence, the transport of sea salt to GvN occurs in the low layers of the atmosphere. Trajectories calculated at the 850 and 925 hPa levels mostly belong to groups 2 and 3, and describe a transport of marine air to GvN.

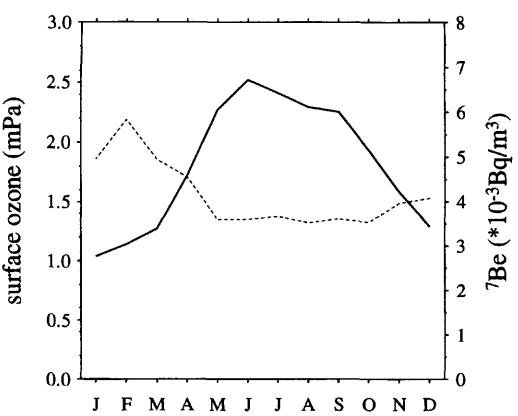

Fig. 10. Annual variability of monthly mean surface ozone partial pressure (solid) and ^{7}Be activity (dashed) during the period 1982–1987.

The annual variability of the monthly averaged sea salt concentration measured at GvN shows maximum values in autumn and a secondary maximum in spring (Fig. 12). The ocean-air flux of sea salt depends on surface wind speed (Eriksson, 1959; Blanchard, 1985; Wu, 1988) and on the sea ice concentration. In summer, the concentration of sea salt is low due to low wind speeds, although the sea ice has its minimum extension. During autumn, the concentration of sea salt increases and reaches its maximum, although the sea ice cover on the ocean increases, too. It is believed that this time the increasing cyclonic activity at GvN is responsible for the growth of sea salt aerosol production and the transport to the coastal station. The cyclonic activity or the mean wind speed has its maximum in the winter time so that the emission of sea salt particles over open water is at a maximum. However, due to the large extention of the sea ice, the sources of sea salt particles are far away of the GvN. Because of the sedimentation of the relatively large sea salt particles, they have only a short atmospheric lifetime and cannot reach the GvN in large numbers. This leads directly to the winter minimum in the time series shown. During spring, a secondary maximum of sea salt is observed, despite the greatest extent of sea ice.

Analysis of the sea ice cover showed that several coastal polynias exist during this season. Trajectories computed during these periods showed a transport of marine air to GvN when a cyclone approached and passed GvN. With decrease of cyclonic activity and strong wind speed

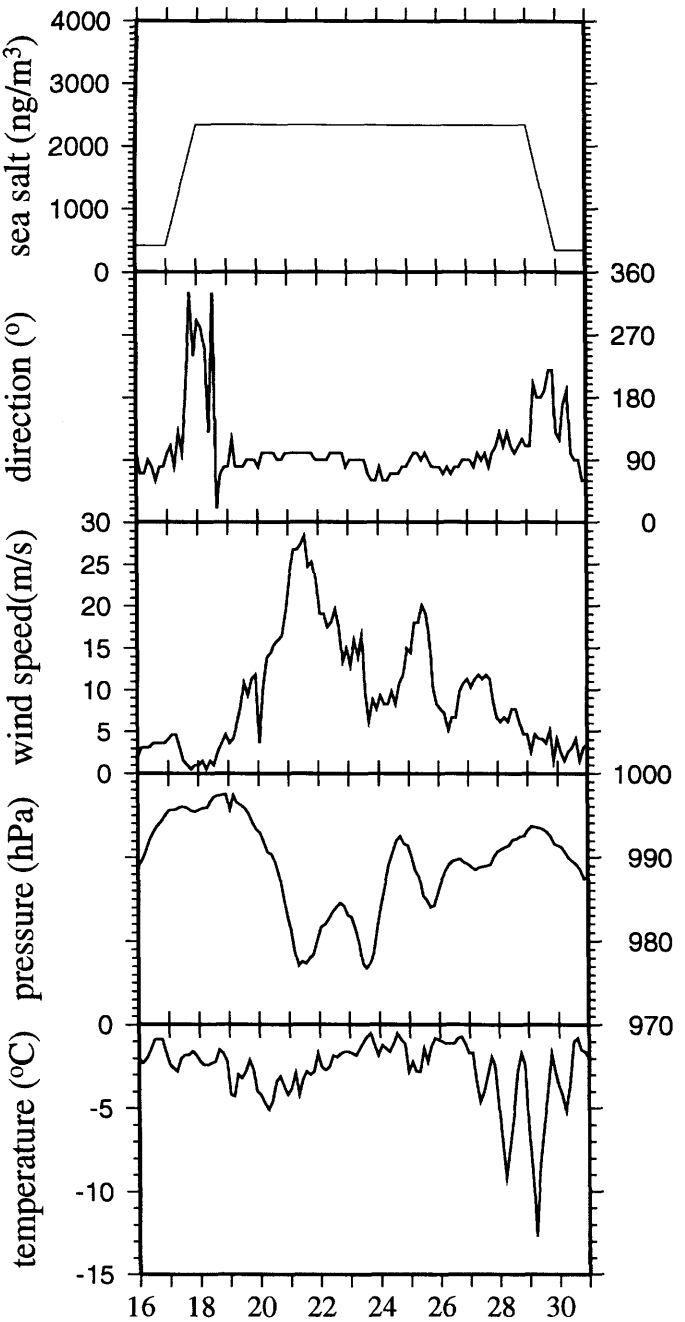

day	850 hPa	925 hPa
18	2	3
19	2	2
20	3	3
21	2	2
22	2	2
23	3	3
24	1	2
25	1	2
26	1	2
27	2	3
28	3	3
29	3	3

Fig. 11. Local meteorological parameters, sea salt density, and trajectories at the 850 and 925 hPa level during the period 16–31 January 1988.

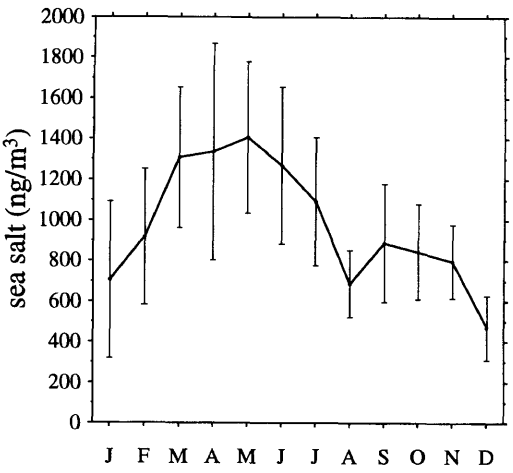

Fig. 12. Annual variability and standard deviation of monthly mean sea salt density during the period 1984–1989.

events in the early summer, sea salt concentrations decrease, in contrast to the melting sea ice. During summer, the potential source of sea salt particles has its maximum area because of the reduced sea ice extent, but the lack of storm events lead to a minimum of the sea salt production over the sea.

5. Conclusions

In this study, the trace elements ^{222}Rn, surface ozone, and sea salt measured at the Antarctic coastal station GvN have been analysed in conjunction with meteorological parameters measured at the same station and trajectories calculated at 500, 850, and 925 hPa levels.

The analysis of daily trajectories calculated for the GvN during 1984–1989 on the 500, 850, and 925 hPa surfaces showed that there are great differences between the flow patterns at different pressure levels. At 500 hPa, westerly flows dominate for 71% of the time, more often in winter than in summer, with an average velocity of 10 ms^{-1}. These situations have the strongest wind speed, which probably cause a vigorous long-range transport of trace elements. Easterly flows occur 29% of the time with an average wind speed of 8 ms^{-1}, more often in summer than in winter due to the migration of the circumpolar trough.

At 850 hPa and 925 hPa, the flows are almost easterly with frequencies of 92% and 97%, respectively. They extend parallel to the coast due to orographic effects. Trajectories coming from the northwest are rare at 850 and 925 hPa, but more often in winter than in summer. Flow patterns from the southwest are totally missing due to the non-presence in the ECMWF wind fields that are used to calculate trajectories.

The flow velocity at 500 hPa has an annual cycle. The weakest transports and therefore the shortest pathways are found in summer. Strongest transports occur from northwesterly directions during winter time. At 850 and 925 hPa, the seasonal variability of the transport velocity is not as pronounced as at the 500 hPa level.

Episodes of high radon concentrations (radon storms) at GvN were in 84% caused by long-range transports of continental air masses from South America to GvN through cyclones. This is observed from the meteorological parameters as well as from the calculated trajectories. In the remaining cases, these radon events were coupled with anticyclonic flows and a transport of air masses from the Antarctic peninsula to GvN.

Strong increases of surface ozone partial pressure also appeared with cyclones approaching GvN. This kind of ozone transport was responsible for 66% of all strong ozone partial pressure increases. A 2nd kind of transport mechanism showed a transport of surface ozone to GvN together with low southerly winds. In these cases, ozone was transported in the middle troposphere southward to Antarctica where the air sinks and flows back northward.

Atmospheric sea salt production depends on wind speed over the ice free ocean and on sea ice cover. Therefore, sea salt events are coupled to strong wind episodes and small sea ice extent. Annual variations of cyclonic activity with strong winds produce sea salt events during autumn. In winter, the extent of sea ice is too large for the transport of sea salt from remote areas to GvN, so that the sea salt concentration has a minimum during winter. The sea salt maxima in spring is caused by polynias that occur near the coast due to break-up processes of the sea ice cover. Together with cyclonic activity, a production and a transport of sea salt particles to GvN becomes possible.

A common feature of all time series of trace elements is a minima of the concentrations during

summer. During this season, cyclonic activity at GvN is rare as seen in the analysis of flow pattern on different pressure surfaces. In summer, anticyclones dominate and a transport of continental clean air occurs more frequently. During autumn and winter, with increasing cyclonic activity, transports from northern areas increase, as does the concentration of trace elements. Minima in the time series are produced by a decrease of sources like the ice cover. During spring, a decrease of trace element concentration can be observed due to the decrease of cyclonic activity that is found in the analysis of trajectories.

6. Acknowledgements

The author is grateful to P. Winkler, Meteorological Observatory Hamburg, and D. Wagenbach, Institute of Environmental Physics in Heidelberg, for the air chemical data. The meteorological data were provided by G. König-Langlo, Alfred Wegener Institute for Polar Research in Bremerhaven. This work has been sponsored by the Deutsche Forschungsgemeinschaft under grant Schl 286/2. All graphs have been plotted with public domain software supplied by Wessel and Smith (1991).

REFERENCES

Attmannspacher, W. 1971. Ein einfaches, naßchemisches Gerät mit geringer Trägheit zur Messung des bodennahen Ozons der Atmosphäre. *Meteorologische Rundschau* **24**, 6, 183–188.

Blanchard, D. C. 1985. The oceanic production of atmospheric sea salt. *J. Geophys. Res.* **90**, 961–963.

Cavalieri, D. J., Gloersen, P. and Campbell, W. J. 1984. Determination of sea ice parameters with the NIMBUS-7 SMMR. *J. Geophys. Res.* **89**, 5355–5369.

Eriksson, E. 1959. The yearly circulation of chloride and sulfur in nature; meteorological, geochemical and pedological implications, Part 1. *Tellus* **11**, 375–403.

Gruzdev, A. N., Elokhov, A. S., Makarov, O. V. and Mokhov, I. I. 1993. Some recent results of Russian measurements of surface ozone in Antarctica. A meteorological interpretation. *Tellus* **45B**, 99–105.

Gube-Lenhardt, M. 1987. The meteorological data of the Georg von Neumayer Station for 1983 and 1984. *Berichte zur Polarforschung* **38**, Alfred-Wegener-Institut, Bremerhaven.

Gube-Lenhardt, M. and Obleitner, F. 1986. The meteorological data of the Georg von Neumayer Station for 1981 and 1982. *Berichte zur Polarforschung* **30**, Alfred-Wegener-Institut, Bremerhaven.

Harris, J. M. 1992. An analysis of 5-day midtropospheric flow patterns for the South Pole: 1985–1989. *Tellus* **44B**, 409–421.

Heintzenberg, J. and Larssen, S. 1983. SO_2 and $SO_4^=$ in the arctic: interpretation of observations at 3 Norwegian arctic-subarctic stations. *Tellus* **35B**, 255–265.

Kahl, J. D., Harris, J. M. and Herbert, G. A. 1989. Intercomparison of three long-range trajectory models applied to Arctic haze. *Tellus* **41B**, 524–536.

Kottmeier, C. 1988. Atmosphärische Strömungsvorgänge am Rande der Antarktis. Habilitationsschrift: *Ber. des Institutes für Meteorologie und Klimatologie der Universität Hannover*, **33**.

Lal, D. and Peters, B. 1967. Cosmic ray produced radioactivity on the earth. *Handbuch der Physik* **46**, S.551–612.

Lambert, G., Polian, G., Sanak, J., Ardouin, B., Buisson, A., Jegou, A, and Le Roulley, J. C. 1982. Radon and daughter products cycle: application to troposphere-stratosphere exchanges. *Ann. Géophys.* **38**, 497–531.

Lambert, G., Ardouin, B. and Sanak, J. 1990. Atmospheric transport of trace elements toward Antarctica. *Tellus* **42B**, 76–82.

Moody, J. L. and Galloway, J. N. 1988. Quantifying the relationship between atmospheric transport and the chemical composition of precipitation on Bermuda. *Tellus* **40B**, 463–479.

Murayama, S., Nakazawa, T., Tanaka, M., Aoki, S. and Kawaguchi, S. 1992. Variations of tropospheric ozone concentration over Syowa Station, Antarctica. *Tellus* **44B**, 262–272.

Oltmans, S. J. 1981. Surface ozone measurements in clean air. *J. Geophys. Res.* **86**, 1174–1180.

Oltmans, S. J. and Komhyr, W. D. 1976. Surface ozone in Antarctica. *J. Geophys. Res.* **81**, 5359–5364.

Pereira, E. B. 1990. Radon-222 time series measurements in the Antarctic peninsula (1986–1987). *Tellus* **42B**, 39–45.

Petterssen, S. 1956. *Weather analysis and forecasting* (ed. S. Petterssen). McGraw-Hill, New York.

Polian, G., Lambert, G., Ardouin, B. and Jegou, A. 1986. Long-range transport of continental radon in subantarctic and antarctic areas. *Tellus* **38B**, 178–189.

Sanak, J., Lambert, G. and Ardouin, B. 1985. Measurements of stratosphere-to-troposphere exchange in Antarctica by using short-lived cosmonuclides. *Tellus* **37B**, 109–115.

Schwerdtfeger, W. 1984. *Weather and climate of the Antarctic* (ed. W. Schwerdtfeger). Elsevier, Amsterdam.

Taljaard, J. J. 1967. Air masses of the southern hemisphere. *Notos* **18**, 79–104.

Turekian, K. K., Nozaki, Y. and Benninger, L. K. 1977. Geochemistry of atmospheric Radon and Radon products. *Ann. Rev. Earth Planet. Sci.* **5**, 227–255.

Wagenbach, D., Görlach, U., Moser, K. and Münnich, K. O. 1988. Coastal Antarctic aerosol: the seasonal pattern of its chemical composition and radionuclide content. *Tellus* **40B**, 426–436.

Wessel, P. and Smith, W. H. F. 1991. Free software helps map and display data. *EOS Transactions AGK* **72**, 441; 445–446.

Wexler, H., Moreland, W. B. and Weyant, W. S. 1960. A premilinary report on ozone observations at Little America, Antarctica. *Mon. Weath. Rev.* **88**, 7312–7330.

Wilkening, M. H. and Clements, W. E. 1975. Radon-222 from the ocean surface. *J. Geophys. Res.* **80**, 3828–3830.

Winkler, P., Brylka, S. and Wagenbach, D. 1992. Regular fluctuations of surface ozone at Georg-von-Neumayer Station, Antarctica. *Tellus* **44B**, 33–40.

Wu, J. 1988. Bubbles in the near-surface ocean: a general description. *J. Geophys. Res.* **93, C1,** 587–590.